*Journal of Statistical Physics, Vol. 57, Nos. 3/4, 1989*

# Long-Time Tails in Lattice Lorentz Gases

**M. H. Ernst**[1] **and G. A. van Velzen**[1]

*Received March 20, 1989*

We consider a Lorentz gas on a square lattice with a fraction $c$ of scattering sites. The collision laws are deterministic (fixed mirror model) or stochastic (with transmission, reflection, and deflection probabilities $\alpha$, $\beta$, and $\gamma$ respectively). If all mirrors are parallel, the mirror model is exactly solvable. For the general case a self-consistent ring kinetic equation is used to calculate the long-time tails of the velocity correlation function $\langle v(0)\, v(t)\rangle$ and the tensor correlation $\langle Q(0)\, Q(t)\rangle$ with $Q = v_x v_y$. Both functions show $t^{-2}$ tails, as opposed to the continuous Lorentz gas, where the tails are respectively $t^{-2}$ and $t^{-3}$. Inclusion of the self-consistent ring collisions increases the low-density coefficient of the tail in $\langle v(0)\, v(t)\rangle$ by 30–100% as compared to the simple ring collisions, depending on the model parameters.

**KEY WORDS**: Lorentz gas; cellular automaton fluids; diffusion; velocity correlation function; long-time tail.

## 1. INTRODUCTION

In this volume honoring E. G. D. Cohen we present a study of time correlation functions and diffusion in Lorentz gases, topics that have had Cohen's long-standing[1] and recent[2] interest. Here these problems are posed in the context of lattice gas cellular automata, which offer many surprising results.

In these models time, positions, and velocities are discretized, and the dynamics is simple in the sense that only particles present in the same cell at time $t$ determine velocities and positions at time $t+1$. The fluid versions of such models are of great practical interest because they are used for large-scale simulations of hydrodynamic flow problems and they provide the basis for the current construction of many dedicated parallel com-

[1] Institute for Theoretical Physics, 3508 TA Utrecht, The Netherlands.



0022-4715/89/1100-0455$06.00/0 

puters. These lattice gases contain much, and hopefully most, of the essential physics of fluids. They also have a more fundamental importance in the sense that they serve as a testing ground for kinetic theory, because the simple dynamics frequently allows a more complete and more detailed kinetic theory analysis.

To illustrate the typical difference between fluids and Lorentz gases, we recall that the velocity autocorrelation function (VACF) $\varphi(t) = \langle v_x(0)\, v_x(t)\rangle$ of a tagged particle in a fluid in thermal equilibrium decays algebraically $\sim t^{-\alpha(d)}$, as was discovered in computer simulations[3,4] and quantitatively explained from kinetic theory[5] and mode coupling theory.[6] The exponent $\alpha(d) = d/2$ for dimensionality $d \geqslant 2$ and $\alpha(1) = 2/3$ for $d = 1$. This long-time tail shows that the coefficient of diffusion $D$, which is given by the long-time limit of $D(t) = \int dt\, \varphi(t)$, does not exist in fluids with dimensionality $d \leqslant 2$. Similar arguments apply to viscosity and heat conductivity. Fluids in two dimensions suffer therefore from the fundamental problem that linear transport coefficients do not exist. Lattice gas cellular automata exhibit the same difficulties.[8]

A Lorentz gas can be considered as a binary fluid mixture of "heavy" and "light" particles. The "heavy" particles are immobile scatterers; the "light" particles are moving ballistically with constant speed $|\mathbf{v}| = 1$, independently of one another. Upon collision with a scatterer, they only change their direction of motion. The collision dynamics may follow deterministic or stochastic rules.[9-11]

Equilibrium time correlation functions have a slightly weaker, but still algebraic tail. By a minor extension of the low-density kinetic theory of ref. 12 one finds

$$\varphi_l(t) = \langle Q_l(0)\, Q_l(t)\rangle \sim A_l t^{-(d/2)-l} \tag{1.1}$$

where $l = 1, 2, 3, \ldots$ labels the spherical harmonics:

$$\begin{aligned} Q_1 &= v_\alpha; \qquad Q_2 = v_\alpha v_\beta - \delta_{\alpha\beta}/d \\ Q_3 &= v_\alpha v_\beta v_\gamma - (v_\alpha\, \delta_{\beta\gamma} + v_\beta\, \delta_{\alpha\gamma} + v_\gamma\, \delta_{\alpha\beta})/(d+2) \end{aligned} \tag{1.2}$$

where $\alpha, \beta, \ldots = x, y, \ldots, d$ label Cartesian components. The basic dynamics causing these long memories are the ring collisions, from which the coefficients $A_l$ can be calculated to lowest order in the density of scatterers. The theoretical predictions for exponents agree reasonably well; the coefficients $A_l$ do not agree well with those measured in computer simulations.[9] However, in a Lorentz gas with a hopping particle (as opposed to the ballistic motion in the previous models) moving on a lattice with excluded bonds or sites, there is very good agreement between theory and computer

simulations to lowest and next order in the densities in leading and subleading time tails.[13,14] The continuous two-dimensional Lorentz gas has a well-defined diffusion coefficient, which behaves for small concentration $c$ of scatterers as $cD(c) = d_0 + d_1 c \ln c + \cdots$.[15] The $\ln(c)$ contribution comes again from the ring collisions. It was one of the fundamental discoveries of Cohen and collaborators[16] to establish the nonanalytic density dependence of transport coefficients in fluids.

The plan of the paper is as follows. In Section 2 the Liouville equation is formulated for several lattice Lorentz gases, and time correlation functions are introduced; in Section 3 the Boltzmann equation and the self-consistent ring equation are solved and the resulting diffusion coefficient is compared with computer simulations. We further discuss an exactly soluble two-dimensional lattice Lorentz gas. The long-time tails are analyzed using the self-consistent ring-kinetic equation in Section 4. The paper concludes with a summary of the most interesting results.

## 2. LIOUVILLE OR CHAPMAN–KOLMOGOROV EQUATION

Consider a square lattice of $N$ sites, a fraction $c$ of which is occupied by scatterers. At the integer-valued time $t = 0, 1, 2, \ldots$ the moving particle is at one of the lattice sites and has a "velocity" $e_1 = (1, 0)$, $e_2 = (0, 1)$, $e_3 = (-1, 0)$, or $e_4 = (0, -1)$. To describe the configuration of scatterers, we assign a random variable $c_n$ to site $n = (n_x, n_y)$, with value $c_n = 1$ for a scattering site and $c_n = 0$ for a nonscattering site.

Let $p_i(n, t)$ denote the probability to find the moving particle at site $n$ with (arrival) velocity $e_i$ [$i = 1, 2, 3, 4 \pmod 4$]; then the Liouville equation (deterministic dynamics) or the Chapman–Kolmogorov equation (stochastic dynamics) reads

$$p_i(n + e_i, t + 1) = (1 - c_n)\, p_i(n, t) + c_n \sum_j W_{ij}(\varphi_n)\, p_j(n, t)$$

$$= p_i(n, t) + c_n \sum_j T_{ij}(\varphi_n)\, p_j(n, t) \tag{2.1}$$

$T(\varphi) = W(\varphi) - 1$ is a $4 \times 4$ collision matrix, where $\varphi_n$ may be an additional site-dependent random or sure variable to specify a type of scatterer. For further details about notation we refer to ref. 17.

There exist many different types of deterministic lattice Lorentz models. Gates[18] considered a model with identical gyral scatterers that rotate the velocity of the particle over an angle of $\pi/2$. Gunn and Ortuño[19] considered a model with three different types of scatterers (specified by the random variable $\varphi_n$) that rotate the velocity over $\pi/2$, $\pi$,

or $3\pi/2$ rad. Such models show a wealth of percolation phenomena. Binder[20] considered *an alternating time model* where a scatterer rotates the velocity over $+\pi/2$ or $-\pi/2$, depending on the parity of time. Here the collision matrix $T(t)$ depends on time. Ruijgrok and Cohen[2] studied the *mirror model*, where the scatterers are fixed mirrors, oriented parallel to $n_x = n_y$ if $\varphi_n = +$ (fraction $f$) and parallel to $n_x = -n_y$ if $\varphi_n = -$ (fraction $1-f$). The matrix $W(\varphi_n)$ is here

$$W_{ij}(+) = \left(\begin{array}{cc|cc} 0 & 1 & & \\ 1 & 0 & & \\ \hline & & 0 & 1 \\ & & 1 & 0 \end{array}\right) \quad \text{and} \quad W_{ij}(-) = \left(\begin{array}{cc|cc} & & 0 & 1 \\ & & 1 & 0 \\ \hline 0 & 1 & & \\ 1 & 0 & & \end{array}\right) \tag{2.2}$$

The authors considered only the case $f = 1/2$, where the diffusion tensor is isotropic. Finally, Ernst *et al.*[17] studied a *stochastic model* where $T = W - 1$ is the same for all scatterers:

$$W_{ij} = \begin{pmatrix} \alpha & \gamma & \beta & \gamma \\ \gamma & \alpha & \gamma & \beta \\ \beta & \gamma & \alpha & \gamma \\ \gamma & \beta & \gamma & \alpha \end{pmatrix} \tag{2.3}$$

with normalization $\alpha + \beta + 2\gamma = 1$. Here $\alpha$, $\beta$, and $\gamma$ represent, respectively, the probability of transmission ($i \to i$), reflection ($i \to i+2$), and deflection ($i \to i \pm 1$).

In a compact notation we represent the conditional probability $P_{ni,mj}(t)$ with initial value $P_{ni,mj}(0) = \delta_{nm}\,\delta_{ij}$ as a $4N \times 4N$ matrix and write the Liouville equation as

$$\begin{aligned} P(t+1) &= S^{-1}[1 + CT(\varphi)]\,P(t) \\ &= \{S^{-1}[1 + CT(\varphi)]\}^t\, S^{-1} \end{aligned} \tag{2.4}$$

where streaming, density, and collision operators are defined as

$$\begin{aligned} S_{ni,mj} &= \delta_{m,n+e_i}\,\delta_{ij} \\ C_{ni,mj} &= c_n\,\delta_{nm}\,\delta_{ij} \\ T_{ni,mj}(\varphi) &= \delta_{nm}\,T_{ij}(\varphi_n) \end{aligned} \tag{2.5}$$

In solving (2.4), we have used $p_i(n + e_i, 1) = p_i(n, 0)$ or $P(1) = S^{-1}$, as the specified velocities are *arrival* velocities. To obtain the mean probabilities

$\langle P(t)\rangle$, one has to average over the distribution of the quenched random variables $\{c_n, \varphi_n\}$.

The quantity of main interest is the VACF, $\varphi(t)=\langle v_x(0)\, v_x(t)\rangle$, which reads in the notation of ref. 17

$$\varphi(t)=\sum_n \langle V_x|\, P_{n0}(t+1)\,|V_x\rangle \tag{2.6}$$

The bras and kets denote 4-vectors. An inner product is defined through $\langle a|b\rangle=\frac{1}{4}\sum_i \langle a_i b_i\rangle$, which also implies the average $\langle\cdots\rangle$ over the quenched variables. The velocity vector is defined as $|V_\alpha\rangle_i=(e_i)_\alpha$ or $|V_x\rangle=(1, 0, -1, 0)$ and $|V_y\rangle=(0, 1, 0, -1)$. We have also used that $\langle P_{nm}\rangle$ depends only on $(n-m)$ because of translational invariance. In a similar fashion one may consider the tensor correlation function $\chi(t)=\langle Q(0)\, Q(t)\rangle$ with $Q=V_x^2-V_y^2$, which can be represented as

$$\chi(t)=\sum_n \langle V_x^2-V_y^2|\, P_{n0}(t+1)\,|V_x^2-V_y^2\rangle \tag{2.7}$$

where $|V_x^2-V_y^2\rangle=(1, -1, 1, -1)$. It is further convenient to introduce the discrete Laplace transform of $\varphi(t)$:

$$\begin{aligned}\Phi(z)&=\sum_{t=0}^{\infty}(1+z)^{-t-1}\,\varphi(t)\\ &=\sum_n \langle V_x|\,\{[(1+z)S-1-CT]^{-1}\}_{n0}\,|V_x\rangle\end{aligned} \tag{2.8}$$

and similarly for the Laplace transform $X(z)$ of $\chi(t)$ in (2.7). Finally, the diffusion coefficient is given by

$$D=\frac{1}{2}\varphi(0)+\sum_{t=1}^{\infty}\varphi(t)=\Phi(0)-\frac{1}{4} \tag{2.9}$$

where $\varphi(0)=\langle V_x|\, V_x\rangle=1/2$.

## 3. BOLTZMANN APPROXIMATION AND RING COLLISIONS

At low concentration of scatterers one expects intuitively that returns of the moving particle to a previously visited scatterer (ring collisions) may be neglected and that only uncorrelated collisions have to be taken into account (Boltzmann approximation). If this assumption were correct, one could replace the average $\langle CTP\rangle$ on the right-hand side of (2.4) by a product of averages, and the equation for the average probability would

reduce to the standard Chapman–Kolmogorov equation for a uniform lattice

$$\langle P(t+1)\rangle = S^{-1}(1-\Lambda^0)\langle P(t)\rangle \tag{3.1}$$

where the Boltzmann collision operator is a $4\times 4$ matrix

$$\Lambda^0 = -\langle C\rangle\langle T\rangle = -c\langle T\rangle \tag{3.2}$$

After some rearrangements the Laplace transform (2.8) of the VACF can be reduced to

$$\Phi(z) = \langle V_x|\,(z+\Lambda^0)^{-1}\,|V_x\rangle \tag{3.3}$$

and a similar expression for the tensor correlation function (2.7). Once eigenvectors and eigenvalues of $\Lambda^0$ are known, $\varphi(t)$ and $\chi(t)$ follow immediately.

In the *stochastic Lorentz model* all scatterers are identical and $\Lambda^0 = -cT = c(1-W)$ with $W$ in (2.3). The matrix $\Lambda^0$ has the same cubic symmetric form as (2.3) with $\alpha$, $\beta$, and $\gamma$ replaced by $\alpha' = c(1-\alpha)$, $\beta' = -c\beta$, and $\gamma' = -c\gamma$, respectively. One easily verifies that $|1\rangle$, $|V_x\rangle$, $|V_y\rangle$, and $|V_x^2 - V_y^2\rangle$ are eigenvectors (where $|1\rangle_i = 1$ for $i = 1, 2, 3, 4$) with eigenvalues respectively given by

$$\begin{aligned}
\lambda_0^0 &= \alpha' + \beta' + 2\gamma' = c(1-\alpha-\beta-2\gamma) = 0\\
\lambda_1^0 &= \lambda_2^0 = \alpha' - \beta' = c(1-\alpha+\beta) = 2c(\beta+\gamma)\\
\lambda_3^0 &= \alpha' + \beta' - 2\gamma' = 4c\gamma
\end{aligned} \tag{3.4}$$

It then follows from (3.3) and (2.9) that the diffusion coefficient $D^0$ of the stochastic Lorentz model in the Boltzmann approximation is given by

$$D^0 = \frac{1}{2\lambda_1^0} - \frac{1}{4} = \frac{1}{4c(\beta+\gamma)} - \frac{1}{4} \tag{3.5}$$

By inserting the Laplace transform (2.8), it follows from (3.3) and (3.4) that the time correlation functions in the Boltzmann approximation are

$$\varphi^0(t) = \tfrac{1}{2}(1-\lambda_1^0)^t, \qquad \chi^0(t) = (1-\lambda_3^0)^t \tag{3.6}$$

If all sites are occupied by scatterers ($c = 1$), then the stochastic Lorentz model reduces to a random walk on a uniform lattice, for which the results (3.1)–(3.6) are *exact*.

For the deterministic *mirror model* defined above (2.2), it follows that the Boltzmann collision operator is

$$\Lambda^0 = -c\langle T\rangle = cf[1-W(+)] + c(1-f)[1-W(-)] \tag{3.7a}$$

or

$$\Lambda^0 = c \begin{pmatrix} 1 & -f & 0 & f-1 \\ -f & 1 & f-1 & 0 \\ 0 & f-1 & 1 & -f \\ f-1 & 0 & -f & 1 \end{pmatrix} \tag{3.7b}$$

In the *isotropic* case ($f = 1/2$), considered by Ruijgrok and Cohen, this matrix has the same cubic symmetric form as in the stochastic case with $\alpha = \beta = 0$ and $\gamma = 1/2$. The eigenvalues are then $\lambda_1^0 = c$ and $\lambda_3^0 = 2c$; the time correlation functions are given by (3.6), and the diffusion coefficient becomes $D^0 = 1/(2c) - 1/4$, as already calculated in ref. 2. In the *anisotropic* case the macroscopic system does not have the full cubic symmetry: it is only invariant under reflections in the lines $n_x = \pm n_y$ and under inversion, but not under discrete rotations. In this case the eigenvectors are $|1\rangle$, $|V_x + V_y\rangle$, $|V_x - V_y\rangle$, and $|V_x^2 - V_y^2\rangle$ with eigenvalues respectively given by

$$\lambda_0^0 = 0; \qquad \lambda_1^0 = 2c(1-f); \qquad \lambda_2^0 = 2cf; \qquad \lambda_3^0 = 2c \tag{3.8}$$

The correlation function $\chi^0(t)$ still has the same form as in (3.6), but the VACF is a tensor

$$\Phi_{\alpha\beta}(z) = \langle V_\alpha | \, (z + \Lambda^0)^{-1} \, | V_\beta \rangle \tag{3.9}$$

with $(\alpha, \beta) = (x, y)$, which can be brought on to the principal axes by the rotation $\xi = (x+y)/\sqrt{2}$ and $\eta = (x-y)/\sqrt{2}$. The resulting VACFs are, for $t = 0, 1, 2, \ldots$,

$$\begin{aligned} \varphi_{\xi\xi}(t) &= \tfrac{1}{2}[1 - 2c(1-f)]^t \\ \varphi_{\eta\eta}(t) &= \tfrac{1}{2}(1 - 2cf)^t \end{aligned} \tag{3.10}$$

and the corresponding anisotropic diffusion coefficients

$$\begin{aligned} D_{\xi\xi}^0 &= (2\lambda_1^0)^{-1} - \tfrac{1}{4} = \tfrac{1}{4}\{1/[c(1-f)] - 1\} \\ D_{\eta\eta}^0 &= (2\lambda_2^0)^{-1} - \tfrac{1}{4} = \tfrac{1}{4}(1/cf - 1) \end{aligned} \tag{3.11}$$

The anisotropic mirror model has a limit, $f \to 1$, or $f \to 0$, as illustrated in Fig. 1, in which the Boltzmann approximation is *exact*. The reason is that returns of the moving particle to the same scatterers are impossible. In the $\xi$ direction the particle moves with a constant velocity $\xi = \xi_0 + t/\sqrt{2}$, so that the mean square displacement is $\langle (\xi - \xi_0)^2 \rangle = t^2/2$, corresponding to a divergent diffusion coefficient $D_{\xi\xi}$. In the $\eta$ direction this deterministic Lorentz model shows diffusive behavior, namely $\langle (\eta - \eta_0)^2 \rangle \simeq 2D_{\eta\eta} t$ for

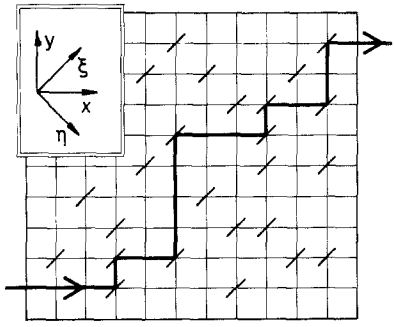


Figure 1

long times, where $D_{\eta\eta} = (1-c)/4c$ is *exact for all values of the concentration c*. Also, the time correlation functions $\varphi^0(t)$ and $\chi^0(t)$ are exact. Except for $\varphi_{\xi\xi}(t) = 1/2$, they decay exponentially for all time. There are no algebraic long-time tails.

The Boltzmann approximation to lattice Lorentz gases does not always yield a simple density dependence for the diffusion coefficient as in (3.5) or (3.11). In the *alternating time model*[20] summation of the uncorrelated collisions yields[21]

$$D^0 = (2-2c+c^2)/[4c(1-c)] \tag{3.12}$$

The diffusion coefficient is proportional to the mean free path $l_0$ between scatterers at low densities ($l_0 \sim 1/c$) or between "holes" at high densities $l_0 \sim 1/(1-c) = 1/p$. At a low concentration of "holes" and for times much shorter than $1/p$, the particle moves along a "staircase."

How good is the Boltzmann approximation? To answer this question we consider first the computer simulations performed by Ruijgrok and Cohen[2] on the Lorentz model with fixed mirrors. These authors measured the density dependence of the diffusion coefficient and found the surprising result that the Boltzmann approximation for the diffusion coefficient $D^0(c) = 1/(2c) - 1/4$ agreed very well with the simulation results at all densities. The more extended simulations of Kong and Cohen[2] show appreciable deviations.

In cellular automaton models for two-dimensional fluids similar good agreement between the Boltzmann equation and simulation results was found for the viscosities,[22] not only at low and high (by duality) density, but also at intermediate densities, notwithstanding the fundamental difficulties in two-dimensional fluids mentioned in the introduction.

In order to understand these unexpected results, we have used a kinetic theory analysis to calculate the contributions from higher order correlated collision sequences. To select the most important collision

sequence, we have used the methods of Hauge and Cohen[1] to make the phase space estimates given in Fig. 2. At small densities the ring-type and orbiting collision sequences have the largest phase space. Furthermore, if the velocity of the moving particle can be reversed in a collision (backscattering, $\beta \neq 0$), then the magnitude of the ring-type contributions is increased by a factor $1/c$ at small densities and becomes of equal size to that of the uncorrelated collision sequences, summed by the Boltzmann equation (see leftside, Fig. 2). This effect is also present in the hard-rod fluid[23] and in a modified version of the Ehrenfest windtree model.[24]

The actual resummation of relevant ring-type collision sequences and the calculation of the diffusion coefficient $D(c)$ for several values of the transmission coefficient $\alpha$, reflection coefficient $\beta$, and deflection coefficient $\gamma$ [see Eq. (2.3)] can be found in ref. 17. These theoretical results are shown in Fig. 3 as solid lines together with the Boltzmann results (dashed lines). The results of extensive computer simulations are indicated by their error bars. One sees that the simulated values of the diffusion coefficient agree well with the Boltzmann values in models without backscattering ($\beta = 0$).

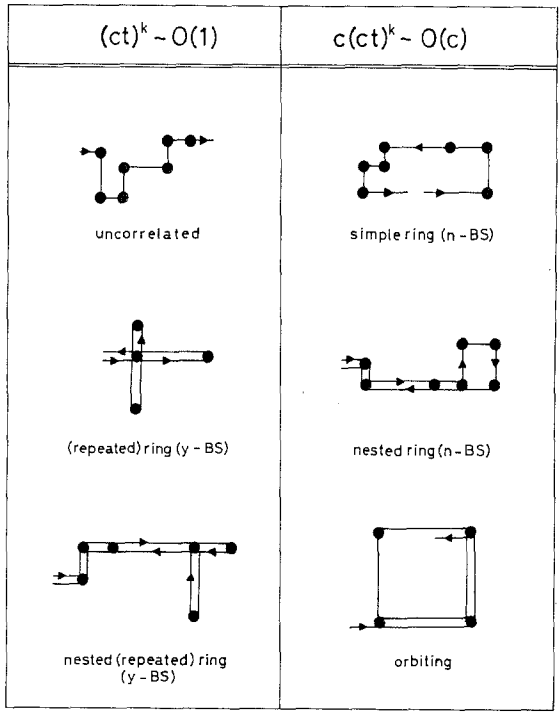


Figure 2

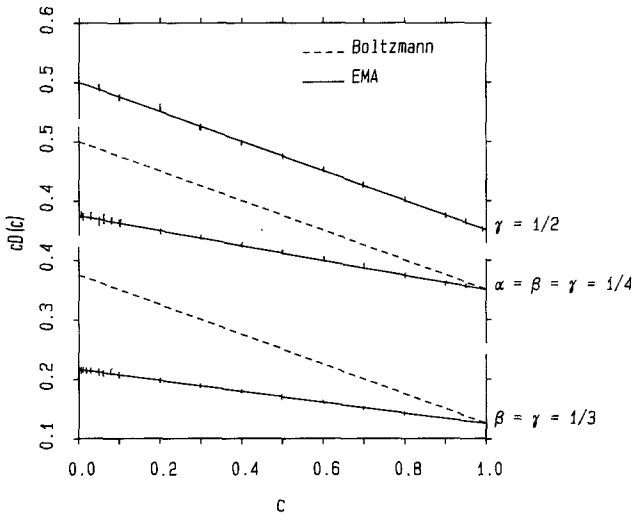


Figure 3

This is shown in the top curve of Fig. 3 for the model with only left or right scattering ($\gamma = 1/2$; $\alpha = \beta = 0$), where $cD^0(c) = \frac{1}{2} - \frac{1}{4}c$ as in the fixed mirror model of Ruijgrok and Cohen. In this case the self-consistent ring equation (solid line) and Boltzmann equation (dashed line) coincide. For the continuous Lorentz gas, van Leeuwen and Weyland[15] have shown that the ring diagrams and the "special" diagrams (a subset of the nested rings) both contribute $O(c \ln c)$ corrections to the Boltzmann value $cD^0(c)$. In our stochastic lattice Lorentz gas with $\gamma = 1/2$ the total contributions from the simple ring and from the nested rings cancel exactly.

In the case of backscattering ($\beta \neq 0$), the (nested) ring diagrams drastically change the low-density behavior of the diffusion coefficient. Also here the theoretical calculations are in excellent agreement with the results of computer calculations, as shown in the two lower solid curves of Fig. 3. The dashed curves show that the Boltzmann equation gives completely incorrect results, even at the lowest densities.

## 4. LONG-TIME TAILS

In view of the success of the self-consistent ring summation for determining the density dependence of the diffusion coefficient, particularly in cases where the Boltzmann equation fails totally, we use the same theory to calculate long-time tails of correlation functions. There are again surprises: in the continuous Lorentz gas the coefficient of the tail in the VACF to lowest order in the density is exclusively determined by the simple ring collisions; in lattice gas models this coefficient is determined by the nested

rings even in cases without backscattering where the diffusion coefficient is still correctly given by its Boltzmann value as $c \to 0$. Furthermore, in the tensor correlation function $\chi(t)$ in (2.7) even the exponent is different from the corresponding tensor correlation function (1.2), $\varphi_2(t) \sim t^{-3}$ in the continuous case.

The derivation will be given for the stochastic Lorentz model, but can be adapted trivially to the fixed mirror model. The basic method is given in ref. 17. Here we only present an outline. We start from the VACF in (2.8) by replacing the site-dependent collision operator $CT$, containing the fluctuating densities $c_n$, by an effective site-independent collision operator $cT^e(z)$, where

$$\delta T_n = c_n T - cT^e(z) \equiv c_n T + \Lambda(z) \tag{4.1}$$

The effective collision operator represents the contributions from collision sequences that we want to resum; e.g., setting $T^e(z) = T$ sums all uncorrelated collision sequences. To determine $T^e(z)$, we expand the exact resolvent $\Gamma(z) = \langle [(1+z)S - 1 - CT]^{-1} \rangle$ in (2.8) around the effective resolvent

$$G(z) = [(1+z)S - 1 + \Lambda(z)]^{-1} \tag{4.2}$$

require that all remaining ring-type contributions to $\Gamma(z)$ vanish identically, and neglect all remaining non-ring-type contributions. This imposes the self-consistency or effective medium condition:

$$\langle \delta T_n / (1 - R\,\delta T_n) \rangle = 0 \tag{4.3}$$

Hence $\Gamma(z) \simeq G(z)$ in the effective medium approximation. The $4 \times 4$ matrix $R(z)$ represents the ring integral

$$R(z) \equiv G_{00}(z) = \int_q [(1+z)e^{iqV} - 1 + \Lambda(z)]^{-1} \tag{4.4}$$

and $\int_q$ denotes an average over the first Brillouin zone

$$\int_q \cdots = (2\pi)^{-2} \int_{-\pi}^{\pi} dq_x \int_{-\pi}^{\pi} dq_y \cdots$$

The ring integral $R(z) = G_{nn}(z) = G_{00}(z)$ is the Laplace transform of the single-site Green's function or "staying probability" $\langle P_{nn}(t) \rangle = \langle P_{00}(t) \rangle$ in the self-consistent ring approximation. On the square lattice the moving particle can only be at its starting position after an even number of time steps. This implies $P_{00}(t) = 0$ for odd times, or equivalently, $R(z) = R(-2-z)$, as can be seen from (4.4) by replacing $q_\alpha (\alpha = x, y)$ by $q'_\alpha = q_\alpha + \pi$. These oscillations persist forever. We have further changed to

Fourier representation, and $V_\alpha$ is a diagonal matrix with elements $(V_\alpha)_{ij} = \delta_{ij}(e_i)_\alpha$. Also note the relation $|V_\alpha\rangle = V_\alpha|1\rangle$ between the kets introduced in (3.4).

In our further analysis it is convenient to write out explicitly the average over $c_n$ in (4.3). Using (4.1), this yields for the self-consistency condition (4.3)

$$\frac{c(T+\Lambda)}{1-R(T+\Lambda)}+\frac{(1-c)\Lambda}{1-R\Lambda}=0 \tag{4.5}$$

where all matrices $\Lambda(z)$, $R(z)$, and $T$ have the cubic symmetric form (2.3) and therefore commute. Its simultaneous set of eigenvectors is

$$\begin{aligned} |\psi_0\rangle &= |1\rangle; & |\psi_1\rangle &= 2^{1/2}|V_x\rangle \\ |\psi_2\rangle &= 2^{1/2}|V_y\rangle; & |\psi_3\rangle &= |V_x^2 - V_y^2\rangle \end{aligned} \tag{4.6}$$

with $\langle\psi_l|\psi_{l'}\rangle = \delta_{ll'}$ $(l, l' = 0, 1, 2, 3)$. The corresponding eigenvalues are denoted by $\lambda_l(z)$, $r_l(z)$, and $t_l$, respectively, where the eigenvalues for $l=1$ and $l=2$ are degenerate. Since $T|1\rangle = 0$ or $t_0 = 0$, Eq. (4.5) implies that $\lambda_0(z) = 0$. The corresponding spectral representation of the matrices is

$$\Lambda(z) = \sum_{l=0}^{3} |\psi_l\rangle\, \lambda_l(z)\, \langle\psi_l|, \qquad \text{etc.} \tag{4.7}$$

The combined equations (4.4) and (4.5) determine the matrix $\Lambda(z)$ or equivalently the eigenvalues $\lambda_l(z)$ for $l=1, 2, 3$. Once they are known, the VACF (2.8) is given by the direct analog of (3.3), i.e.,

$$\Phi(z) = \langle V_x|\,[z+\Lambda(z)]^{-1}\,|V_x\rangle = \tfrac{1}{2}[z+\lambda_1(z)]^{-1} \tag{4.8}$$

and similarly for the tensor correlation function $\chi(t)$ in (2.7), i.e.,

$$X(z) = [z+\lambda_3(z)]^{-1} \tag{4.9}$$

To determine the long-time tails we need the dominant small-$z$ singularity of $R(z)$. We use in general the convention that $\delta A(z)$ denotes (the term containing) the dominant small-$z$ singularity of $A(z)$, and $A = A(0)$ denotes the dominant regular part. There are two sources of singular terms in (4.4): The effective collision operator has a singular contribution $\delta\Lambda(z)$ and the ring integral with $\Lambda(z)$ replaced by $\Lambda = \Lambda(0)$ has the standard ring singularity of $O(z \ln z)$. This yields

$$\delta R(z) = \delta \int_q [(1+z)e^{iqV} - 1 + \Lambda]^{-1} - \int_q g\, \delta\Lambda(z)\, g \tag{4.10}$$

where $g = [\exp(iqV) - 1 + A]^{-1}$. The small-$z$ singularity of the first term on the rhs is obtained in essentially the same way as in ref. 12; i.e., we determine the diffusive eigenmode

$$[(1+z)e^{iqV} - 1 + A]\,|\Psi_D(q)\rangle = [z + \omega(q,z)]\,|\Psi_D(q)\rangle \tag{4.11}$$

for small $q$ and $z$, where $\omega(q,z) \simeq Dq^2$ with $D = (2\lambda_1)^{-1} - 1/4$ and $\Psi_D(q) \simeq 1 - iqV/\lambda_1 + \cdots$. We then obtain for the eigenvalue of (4.10)

$$\delta r_l(z) = \langle \psi_l |\, \delta R(z)\, |\psi_l\rangle = \delta_l(z) - \sum_{l'=1}^{3} A_{ll'}\, \delta\lambda_{l'}(z) \tag{4.12}$$

In the last term we have used the spectral representation (4.7) for $\delta A(z)$ and introduced

$$A_{ll'} = \int_q (\langle \psi_l |\, g\, |\psi_{l'}\rangle)^2 \equiv \int_q g_{ll'}^2 \tag{4.13}$$

The first term is, for small $z$,

$$\begin{aligned} \delta_l(z) &= \delta \int_q (\langle \psi_l |\, \Psi_D(q)\rangle)^2/(z + Dq^2) \\ &= \begin{cases} -\pi(4\pi\lambda_1 D)^{-2}\, z \ln z, & l = 1, 2 \\ O(z^2 \ln z), & l = 3 \end{cases} \end{aligned} \tag{4.14}$$

Equation (4.12) gives a linear relation between $\delta r$ and $\delta\lambda$. A second relation can be obtained by applying (4.5) to the eigenvectors (4.6), which yields $r(z) = [\lambda(z) + ct]/\{\lambda(z)[\lambda(z) + t]\}$ for $l = 1, 2, 3$. The leading singularities are therefore related by

$$\frac{\delta r(z)}{\delta\lambda(z)} = -\frac{\lambda^2 + 2ct\lambda + ct^2}{\lambda^2(\lambda + t)^2} \equiv -\alpha(\lambda) \tag{4.15}$$

for $\lambda_l$, $r_l$, $t_l$, and $\alpha_l = \alpha_l(\lambda_l)$ with $l = 1, 2, 3$. All coefficients on the rhs are taken at $z = 0$. With the help of this relation, $\delta r_l(z)$ can be eliminated from (4.12) to yield two coupled linear equations for $\delta\lambda_1(z) = \delta\lambda_2(z)$ and $\delta\lambda_3(z)$. We note two interesting points: first, since $A_{13}$ in (4.12) is in general non-vanishing, one sees that $\delta\lambda_l(z) = -\delta_1(z) a_l$ (with $l = 1, 3$), where $a_l$ follows from these linear equations. This leads to $t^{-2}$ tails in the time correlation functions (4.3) and (4.9), whereas the (not self-consistent) simple ring integral—given by the first term on the rhs of (4.10) and (4.12)—would yield $\varphi(t) \sim t^{-2}$ and $\chi(t) \sim t^{-3}$ as in (1.2). Second, even in the limit of small density, the coupling constant $A_{13}$ between the two equations does not

vanish, but remains of the same order in density as $\alpha_1 \sim \alpha_2 \sim 1/c$ and both tails survive.

Having determined the $\delta\lambda_l(z)$, we determine the dominant small-$z$ singularity in the VACF (4.8) as $\delta\Phi(z) = -\delta\lambda_1(z)/2\lambda_1^2 = (a_1/2\lambda_1^2)\,\delta_1(z)$. According to a Tauberian theorem, $z \ln z$ at small $z$ corresponds to $1/t^2$ at large $t$. Hence, the long-time tail in the VACF is

$$\varphi(t) \simeq -(a_1/2\lambda_1^2)\,\pi(4\pi\lambda_1 Dt)^{-2} \equiv Ec^{-1}t^{-2} \tag{4.16}$$

Similarly, we find for the tail in the correlation function in (4.9)

$$\chi(t) = -(a_3/\lambda_3^2)\,\pi(4\pi\lambda_1 Dt)^{-2} \equiv Fc^{-1}t^{-2} \tag{4.17}$$

Analytic results can be obtained in the low-density limit, as shown for the eigenvalues $\lambda_l$ and the diffusion coefficient in ref. 17. Using similar methods, we have also evaluated the dominant low-density behavior of $A_{ll'}$ analytically:

$$\begin{aligned} A_{11} &= \tfrac{1}{4}(\lambda_3/2\lambda_1^3)^{1/2} \\ A_{13} &= -\tfrac{1}{4}(2\lambda_1\lambda_3)^{-1/2} \\ A_{33} &= \tfrac{1}{2}(\lambda_1/2\lambda_3^3)^{1/2} \\ A_{12} &= (1/8\pi)(\lambda_3/\lambda_1) \end{aligned} \tag{4.18}$$

The first three terms are of $O(1/c)$, since $\lambda_l = O(c)$; the last one is of $O(1)$ and may be neglected. At high densities ($p = 1 - c \to 0$) all integrals remain finite, except for the special case with left or right scattering ($\gamma = 1/2$). Here $A_{33} = (2\pi p)^{-1}$ and $A_{13} = \pi^{-1} \ln p$, whereas $A_{11}$ and $A_{12}$ are finite.

For finite densities we have numerically evaluated all integrals $A_{ll'}$ in (4.13) and calculated $E$ and $F$, defined in (4.17). The eigenvalues $\lambda_1$ and $\lambda_3$ and the diffusion coefficient were obtained numerically in ref. 17. In Fig. 4 the coefficients $E$ and $F$ are plotted as a function of the density for the stochastic models with only left or right scattering ($\gamma = 1/2$, $\alpha = \beta = 0$) and for two models with backscattering ($\alpha = \beta = \gamma = 1/4$) and ($\beta = \gamma = 1/3$; $\alpha = 0$). At high densities the tails vanish: because $\alpha_l \sim O(1/p)$ in (4.15), one can verify directly from (4.12) that the tail amplitudes behave as $E \sim a_1 \sim O(p)$ and $F \sim a_3 \sim O(p^2)$ for small $p = 1 - c$. The stochastic Lorentz model for $c = 1$ represents a random walk for which the exponential forms (3.6) are exact. The high-density results do not apply to the mirror model, for which the relations (4.5) and (4.15) are very different.

In the *low-density limit* we find for the tails of the time correlation functions

$$\begin{aligned} \varphi(t) &\simeq -K(8\pi ct^2)^{-1} \\ \chi(t) &\simeq +L(8\pi ct^2)^{-1} \end{aligned} \tag{4.19}$$

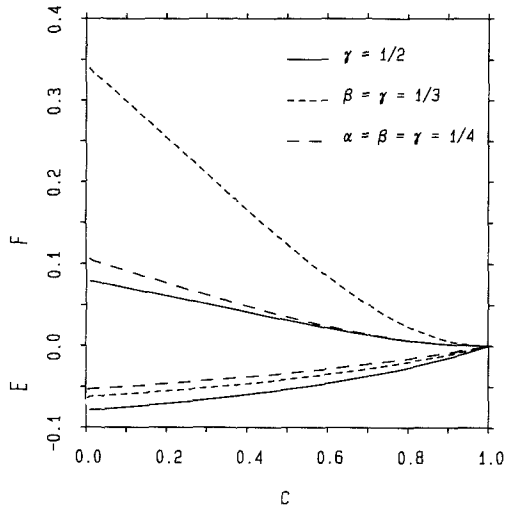


Figure 4

where

$$K = [1 - \tfrac{1}{4}(2b_1b_3)^{1/2}]/[1 - (3/8)(2b_1b_3)^{1/2}]$$
$$L = b_1^2/[(2b_1b_3)^{1/2} - (3/4)\, b_1b_3] \tag{4.20}$$

with $\lambda_l \equiv cb_l$ and we have used the low-density relation $2\lambda_1 D = 1$. Only in cases without backscattering ($\beta = 0$) do the eigenvalues $\lambda_l$ for $l = 1, 2, 3$ approach the corresponding Boltzmann values $\lambda_l^0$ given in (3.4). In cases with backscattering ($\beta \neq 0$) the eigenvalues approach very different low-density limits, which have been calculated in ref. 17, and are listed in Table I for the backscattering models ($\gamma = \beta = 1/3$; $\alpha = 0$) and ($\gamma = \beta = \alpha = 1/4$) together with the numerical values for the coefficients $K$ and $L$. If we would have calculated the tail of the VACF at low densities

**Table I. Coefficients in (4.20)**

| | $b_1 = \lambda_1/c$ | $b_3 = \lambda_3/c$ | $K$ | $L$ |
|---|---|---|---|---|
| $\gamma = 1/2$ | 1 | 2 | 2 | 2 |
| $\gamma = \beta = 1/3$ | $4/\sqrt{3}$ | $4(2/\sqrt{3} - 1)$ | 1.58 | 8.62 |
| $\gamma = \beta = \alpha = 1/4$ | 4/3 | 2/3 | 4/3 | 8/3 |

in the standard fashion from the ring collision integral $R^0(z)$ in (4.4) with $\Lambda(z)$ replaced by the Boltzmann value $\Lambda^0$ in (3.2), then we would have obtained the result (4.19) with $K=1$. Note that ref. 12 yields for the continuous two-dimensional Lorentz gas $\langle v_x(0)\, v_x(t)\rangle \simeq (8\pi n t^2)^{-1}$, where $n$ is the number density of scatterers.

To conclude, we summarize the most important points about time correlation functions and the diffusion coefficient in lattice Lorentz gas models.

(i) For the mirror model, defined in Fig. 1, the *Boltzmann approximation is exact for all density of scatterers c*; time correlation functions decay exponentially for all times.

(ii) For the stochastic Lorentz models, defined in (2.1) and (2.3), with backscattering ($\beta \neq 0$) the *diffusion coefficient at low densities is not given by the Boltzmann equation* (see Fig. 3). This illustrates the subtle limits involved in interchanging the *limit* $c \to 0$ with the *integration* over wave vectors in calculating the eigenvalues of the ring matrix $R(z)$ in (4.4).

(iii) The inclusion of nested ring diagrams in models *with* and *without* backscattering in a self-consistent manner *substantially increases the tail amplitude of the VACF* from a value $K=1$ for the (not self-consistent) simple ring collisions to a renormalized low-density value $K=2$ in the left-right scattering model ($\gamma = 1/2$); $K \simeq 1.58$ in the model ($\beta = \gamma = 1/3$; $\alpha = 0$) and to $K = 4/3$ in the isotropic scattering model ($\alpha = \beta = \gamma = 1/4$). With the help of the present method, similar results can be obtained for the tails in the fixed mirror model of Ruijgrok and Cohen.

(iv) In the continuous Lorentz gas the tail coefficient of the VACF at low densities, as obtained from computer simulations,[9] is about $K_{\text{sim}} \simeq 1.5$–$2$, compared to the ring value $K=1$ in ref. 12. It is therefore of interest to perform a similar self-consistent analysis of nested ring diagrams for the continuous Lorentz gas to try to resolve this 15-year-old controversy between $K$ values obtained from simulations[9] and low-density kinetic theory.[12]

(v) These ideas can also be tested by performing computer simulations of the tensor correlation function $\varphi_2(t) = \langle v_x(0)\, v_y(0)\, v_x(t)\, v_y(t)\rangle$ for the continuous Lorentz gas. The present analysis suggests the possibility that $\varphi_2(t)$ would have a (positive) long-time tail $\sim t^{-2}$ instead of $t^{-3}$ as (1.2), with an amplitude of about the same magnitude as in the (negative) tail of the VACF. Of course, the $t^{-3}$ tail is still present and may be dominant at intermediate times.

(vi) On square lattices time correlation functions, $f(t)$, may contain an oscillatory component of period 1, that persists forever [21]. Our

asymptotic results for long time tails refer only to the coarse grained time dependence, $\bar{f}(t)$. For the present case one may take $\bar{f}(t) = [f(t) + f(t+1)]/2$.

## ACKNOWLEDGMENTS

It is a pleasure to acknowledge stimulating discussions with T. W. Ruijgrok and E. G. D. Cohen. The work of one of us (G. A. v. V.) is financially supported by the Stichting voor Fundamenteel Onderzoek der Materie (FOM), which is sponsored by NWO.

## REFERENCES

1. E. G. D. Cohen, *Theories cinetiques classiques et relativistes*, Colloques Internationaux CNRS, no. 236; E. N. Hauge and E. G. D. Cohen, *J. Math. Phys.* **10**:397 (1969).
2. T. W. Ruijgrok and E. G. D. Cohen, *Phys. Lett.* **133A**:415 (1988); X. Kong and E. G. D. Cohen, *Phys. Rev. B* (1989).
3. B. J. Alder and T. E. Wainwright, *Phys. Rev. A* **1**:18 (1970).
4. T. T. Erpenbeck and W. W. Wood, *Phys. Rev. A* **32**:23 (1985).
5. J. R. Dorfman and E. G. D. Cohen, *Phys. Rev. A* **6**:776 (1972); **12**:292 (1975).
6. M. H. Ernst, E. H. Hauge, and J. M. J. van Leeuwen, *Phys. Rev. A* **4**:2055 (1971); *J. Stat. Phys.* **15**:7 (1976).
7. Y. Pomeau and P. Resibois, *Phys. Rep.* **19C**:69 (1975).
8. L. Kadanoff, G. McNamara, and G. Zanetti, *Phys. Rev. A* (1989).
9. B. J. Alder and W. E. Alley, *J. Stat. Phys.* **19**:341 (1978); *Physica* **121A**:523 (1983).
10. M. H. Ernst and H. van Beijeren, *J. Stat. Phys.* **26**:1 (1984).
11. H. van Beijeren, *Rev. Mod. Phys.* **54**:195 (1982).
12. M. H. Ernst and A. Weijland, *Phys. Lett.* **34A**:39 (1971).
13. J. J. Brey, J. Gomez Ordonez, and A. Santos, *Phys. Lett.* **127A**:5 (1988).
14. D. Frenkel, *Phys. Lett.* **121A**:385 (1987); private communication (January 1989).
15. J. M. J. van Leeuwem and A. Weijland, *Physica* **36**:457 (1967); **38**:35 (1968).
16. E. G. D. Cohen, *Statistical Mechanics at the Turn of the Decade* (Marcel Dekker, New York, 1971), p. 33.
17. M. H. Ernst, G. A. van Velzen, and P. M. Binder, *Phys. Rev.* **39A**:4327 (1989); M. H. Ernst and G. A. van Velzen, *J. Phys. A: Math. Gen.* (1989), to appear.
18. D. J. Gates, *J. Math. Phys.* **13**:1005, 1315 (1972).
19. J. M. F. Gunn and M. Ortuño, *J. Phys. A: Math. Gen.* **18**:L1035 (1985).
20. P. M. Binder, *Complex Systems* **1**:559 (1987); M. H. Ernst and P. M. Binder, *J. Stat. Phys.* **51**:981 (1988).
21. P. M. Binder and M. H. Ernst, *Physica A* (1989), submitted.
22. D. d'Humieres and P. Lallemand, *Complex Systems* **1**:599 (1987); M. Henon, *Complex Systems* **1**:763 (1987); J. P. Rivet, *Complex Systems* **1**:839 (1987).
23. J. L. Lebowitz and J. K. Percus, *Phys. Rev.* **155**:122 (1967); J. L. Lebowitz, J. K. Percus, and J. K. Sykes, *Phys. Rev.* **171**:224 (1968).
24. E. H. Hauge, in *Transport Phenomena*, G. Kirczenow and J. Marro, eds. (Springer-Verlag, 1974), p. 338.